PNAS RESEARCH ARTICLE | MEDICAL SCIENCES

Variable transduction of thyroid hormone signaling in structures of the mouse brain

Richárd Sinkó[a,1], Federico Salas-Lucia[b,1], Petra Mohácsik[a], Emese Halmos[a,c], Gábor Wittmann[d], Péter Egri[a], Barbara M. L. C. Bocco[b], Alice Batistuzzo[b], Tatiana L. Fonseca[b], Csaba Fekete[d], Antonio C. Bianco[b,2], and Balázs Gereben[a,2]

Affiliations are included on p. 9.

Edited by Donald Pfaff, Rockefeller University, New York, NY; received August 7, 2024; accepted December 31, 2024

L-thyroxine (L-T4) monotherapy is the standard treatment for hypothyroidism, administered daily to normalize TSH levels. Once absorbed, T4 is converted to T3 to alleviate most symptoms. However, this treatment abnormally elevates plasma T4 levels in over 50% of patients. Using L-T4-treated Thyroid Hormone (TH) Action Indicator mice, which express a T3-regulated luciferase (Luc) reporter, we examined whether these T4 elevations disrupt TH signaling. Hypothyroid mice exhibited reduced Luc expression across brain regions, and L-T4 treatment failed to restore T3 signaling uniformly. There was also variability in the activity of type 2 deiodinase (D2), the enzyme that generates most brain T3. Intracerebroventricular T4 administration achieved higher elevation of Luc expression in the mediobasal hypothalamus compared to the cortex, and studies on cultured cortical astrocytes and hypothalamic tanycytes revealed cell-type-specific responses to T4. In tanycytes, exposure to T4 sustained D2 activity, leading to progressive T3 signaling, whereas in astrocytes, T4 exposure triggered a drop in D2 activity, limiting T3 production through a ubiquitin-dependent, self-limiting mechanism. The sustained D2 activity in tanycytes was linked to rapid deubiquitination by USP33, as confirmed using a ubiquitin-specific protease (USP) pan-inhibitor and USP33 knockout mice. In conclusion, the brain's response to L-T4 treatment is heterogeneous, influenced by cell-specific regulation of D2-mediated T3 production. While cortical astrocytes exhibit limited T3 signaling due to D2 ubiquitination, tanycytes coexpressing USP33 amplify T3 signaling by rescuing ubiquitinated D2 from proteasomal degradation. These findings provide mechanistic insights into the limitations of L-T4 therapy and highlight the need for tailored approaches to managing hypothyroidism.

thyroid hormone | brain | deiodinase | hypothyroidism | L-T4 supplementation

Significance

Hypothyroidism affects tens of millions globally, with the standard treatment involving levothyroxine (T4) tablets. This approach relies on the enzymatic activation of T4 prohormone into T3 by the D2 enzyme. However, a significant proportion of T4-treated patients continue to experience persistent symptoms. Our study reveals that T4 therapy fails to restore T3-dependent actions across various brain structures, potentially explaining these residual symptoms. This phenomenon arises because the conversion of T4 to T3 can be self-limiting due to cell-type-specific regulation of the D2 enzyme, particularly in cases of elevated T4 levels commonly observed in T4-treated patients. These findings offer valuable mechanistic insights into the limitations of T4 therapy and underscore the need for a more nuanced approach to managing hypothyroidism.

The standard treatment for hypothyroidism involves the daily use of levothyroxine (L-T4) tablets, which successfully normalize serum thyrotropin (TSH) levels and resolve symptoms in the majority of patients. However, a subset of patients, even with appropriate treatment, may continue to experience persistent symptoms, particularly affecting cognition, mood, and overall quality of life (1, 2). Research conducted in both Europe and the United States suggests that approximately 10 to 20% of L-T4-treated individuals report lingering cognitive issues, often described as "brain fog" (3). While non-thyroid-related factors could contribute to these unresolved symptoms, there is growing evidence that incomplete restoration of thyroid hormone (TH) balance and action within the brain may play a significant role. The failure to fully normalize TH signaling in specific brain regions could explain why some patients continue to experience cognitive difficulties despite achieving normal TSH levels (2, 4).

The human brain is highly sensitive to subtle changes in TH signaling, which rapidly influence the expression of T3-responsive genes (5). TH plays a vital role in brain development and continues to impact brain function throughout life (6–8). Despite this, understanding the mechanisms that regulate TH signaling remains challenging due to the brain's complex structure and the specialized functions of its diverse cell types (9, 10). While neurons are considered the primary targets for TH action in the brain, glial cells also play a key role by modulating the delivery of TH to neurons through selective transport and metabolic processes (11, 12). This involves a coordinated system of TH membrane transporters, nuclear receptors (TRs), and transcriptional coregulators. Among these regulatory mechanisms, the deiodinase enzymes, particularly type 2 deiodinase (D2), are essential. D2 locally converts T4 into the active form, T3, and is responsible for producing the majority of T3 that binds to TRs in the brain, ensuring precise TH signaling within neural cells (13).

Author contributions: A.C.B. and B.G. designed research; R.S., F.S.-L., P.M., E.H., G.W., P.E., B.M.L.C.B., A.B., T.L.F., C.F., A.C.B., and B.G. performed research; R.S., F.S.-L., P.M., G.W., P.E., C.F., A.C.B., and B.G. analyzed data; and R.S., F.S.-L., P.M., C.F., A.C.B., and B.G. wrote the paper.

Competing interest statement: A.C.B. is a consultant for AbbVie, Acella, Aligos, Synthonics. The other authors have nothing to disclose.

This article is a PNAS Direct Submission.

[1]R.S. and F.S.-L. contributed equally to this work.

[2]To whom correspondence may be addressed. Email: acbianco@utmb.edu or gereben.balazs@koki.hun-ren.hu.

This article contains supporting information online at https://www.pnas.org/lookup/suppl/doi:10.1073/pnas.2415970122/-/DCSupplemental.

Published February 4, 2025.

The expression of the gene encoding D2 (*Dio2*) in the brain is restricted to extrahypothalamic astrocytes and hypothalamic tanycytes, where it plays distinct roles. Astrocyte-generated T3 exits the cells and it is taken up by neighboring neurons where it acts both paracrinally and is axonally transported to other extrahypothalamic regions to regulate gene expression (10, 14, 15). Typically, astrocytic D2 ensures TH homeostasis. As an example, a mouse in which the *Dio2* has been inactivated selectively in glial cells exhibits a hypothyroid-like mood and cognitive phenotype (16). In contrast, tanycyte-generated T3 is specifically taken up by axons of the hypophysiotropic thyrotropin-releasing hormone (TRH)-secreting neurons that regulates the HPT axis, or transported to the anterior pituitary gland through the venous portal system (10, 15, 17). In both locations, it transduces changes in plasma T4 that are used to regulate TRH and TSH expression, ultimately defining the circulating TH levels (17–19). Thus, while astrocytic D2 is critical for maintaining the physiological function of extrahypothalamic, e.g., cortical and hippocampal neuronal circuits, D2 produced in tanycytes is critical component of the TH-evoked negative feedback regulation of the HPT axis (7).

D2-mediated activation of T4 to T3 triggers a self-limiting mechanism that inactivates D2 through ubiquitination (20), i.e., D2+T4 → Ub-D2+T3+I, and eventual hydrolysis of Ub-D2 in the proteasomes. This mechanism adjusts (stabilizes) T3 production in the face of variable levels of T4. For example, during iodine deficiency (21) or hypothyroidism (22) T3 levels remain relatively stable despite a drop in circulating T4. This is because the lower T4 levels prolong the D2 half-life and allows for an accelerated T4 to T3 conversion. However, this homeostatic behavior of D2 is inconsistent with its role in the TSH feedback mechanism. Indeed, we recently discovered that in the pituitary gland, there is only minimal adjustment of D2 activity across a broad range of T4 levels (23).

That the behavior of D2 (in response to fluctuations in T4 levels) varies in different cell types according to their anatomical location opened a unique perspective into the role played by deiodinases in TH homeostasis. It is conceivable that the underlying mechanisms of T4-induced D2 ubiquitination are cell specific and define the variable transduction of T4 signaling also in hypothalamic tanycytes and extrahypothalamic astrocytes of the brain. While such behavior would explain the basis for the T4-mediated TSH feedback mechanism, it would also set the stage for an uneven D2-mediated TH signaling in tissues where D2 plays a role in defining T3 content such as the brain. This is particularly important for L-T4-treated patients who frequently exhibit high levels of T4 in the circulation (24), possibly explaining their residual cognitive symptoms.

To address these hypotheses, here we used mouse and cell models and confirmed that the effectiveness of T4-induced D2 ubiquitination is cell specific and that restoring TH signaling to the hypothyroid brain with L-T4 does not occur homogeneously. Depending on the L-T4 dose, different brain structures of the same mouse exhibit signs of hypo- or euthyroidism, or eu- and hyperthyroidism. These findings carry broad implications for the use of L-T4-containing therapies for patients with hypothyroidism.

Results

Hypothyroidism and Treatment with L-T4 Structure-Specifically Affect T3-Signaling in the Brain. To study TH signaling in the brain, we took advantage of the TH Action Indicator (THAI) mouse, which expresses a transgene that allows for the measurement of tissue TH action through a T3-regulated luciferase (*Luc*) reporter system (10, 17, 25). This model is particularly suitable for studying D2-mediated T3 signaling in the brain as the *Luc* reporter responds to T3 in a dose-dependent manner (10) and does not respond to T4 (*SI Appendix*, Fig. S1).

Hypothyroid THAI mice were treated with daily doses of L-T4 (1.7 or 1.9 μg/100 g BW/day via gavage) for 2 wk (Fig. 1*A*). Treatment with 1.7 μg L-T4/100 g BW/day normalized serum TSH levels while serum T4 levels remained relatively high and serum T3 levels were around 30% lower than control values (Fig. 1*B*). Higher doses of L-T4 (1.9 μg/100 g BW) further reduced serum TSH levels by ~50% without affecting serum T4 or T3 levels (Fig. 1*B*). This mouse model mimics the profile of thyroid function tests (i.e., normal serum TSH with slightly elevated serum T4 levels and low/normal serum T3 levels) that is frequently observed in L-T4-treated patients with hypothyroidism (26).

After the treatment with L-T4 was complete, the cerebral cortex, cerebellum, hippocampus, and striatum of these mice were processed for *Luc* messenger RNA (mRNA) expression (Fig. 1*C*). The untreated hypothyroid brain exhibited a pronounced reduction in TH signaling in the striatum (~77%), trailed by the cerebellum (~66%), the hippocampus (~54%), and the cerebral cortex (~29%). Treatment with the lower dose of L-T4 restored TH signaling to the euthyroid levels in all brain areas, except for the cerebellum, which remained ~39% below euthyroid controls (Fig. 1*C*). Higher doses of L-T4 normalized TH signaling in the cerebellum but led to a further increase in TH signaling in the cerebral cortex,

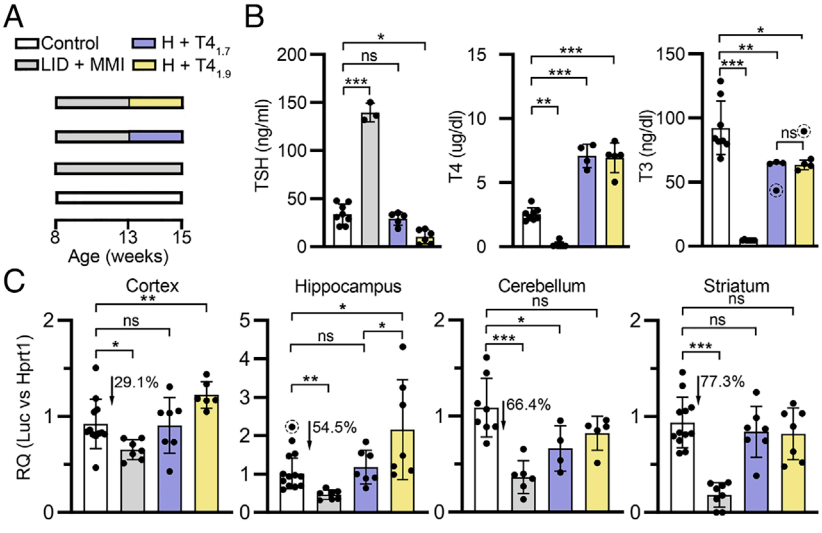

Fig. 1. Treatment with L-T4 does not restore T3 signaling homogeneously in the hypothyroid brain of THAI mice. (*A*) The diagram shows the experimental groups studied; colored horizontal bars show different treatments. (*B*) Plasma TSH, T4, and T3 in mice undergoing the indicated treatment. (*C*) *Luc* mRNA levels in the indicated areas and treatments. Values are mean ± SD of 3 to 10 independent experiments; Values identified as outliers (Q10%) are indicated with a dashed circle. One-way ANOVA and the Tukey post hoc test were used for multiple comparisons; **P* < 0.05, ***P* < 0.01, ****P* < 0.001; ns: nonsignificant; LID: low iodine diet, MMI: methimazole, TSH: thyrotropine, T4: serum thyroxine, T3: serum triiodothyronine, H + $T4_x$: hypothyroid treatment + T4 treatment indicated by x. RQ: relative quantity, *Luc*: luciferase mRNA, *Hprt1*: hypoxanthine phosphoribosyl transferase 1 mRNA.

above what was observed in the control mice. In the other brain areas, TH signaling remained similar to intact control levels (Fig. 1*C*).

The results revealed marked heterogeneity in T3 signaling among different brain areas in their response to hypothyroidism and treatment with L-T4. On the one hand, the striatum and cerebellum are the structures most affected by hypothyroidism, i.e., less capable of mitigating the low serum T4 and T3 levels, which is in contrast to the well-developed ability of the cerebral cortex to preserve TH signaling during hypothyroidism. This is in agreement with the cerebral cortex's exquisite sensitivity to L-T4 administration: T3-signaling was normalized with the lower dose of L-T4, while the higher dose of L-T4 caused a slight increase in TH signaling (Fig. 1*C*).

D2-Mediated T4 Activation Is Brain Structure Specific. Treatment with L-T4 affects TH signaling in the brain by i) the local activation of T4 to T3 via D2 and ii) the systemical activation of T4 to T3 via D1 and D2, which will then enter the brain through the blood–brain barrier and trigger TH signaling. Because in our experimental mouse model the circulating T3 levels were similar between the lower and higher doses of L-T4 (Fig. 1*B*), we considered that the brain heterogeneity in the response to L-T4 treatment was caused by variable transduction of the T4 signaling via the D2 pathway. Mechanistically, this could be explained by differences in the process of T4-induced loss of D2 activity (20), which limits how much T3 is produced within a certain brain structure. A strong loss of D2 would greatly limit T4-mediated T3 signaling, whereas the opposite would be observed in areas where T4-induced loss of D2 is not an active pathway.

To test whether this was the case, we treated hypothyroid mice with a single injection of L-T4 (2.5 μg *i.p*; Fig. 2*A*) and killed them 8 h later. This was sufficient to trigger modest T3 signaling, given that TSH levels were only reduced by ~31% when compared to PBS-treated hypothyroid mice (Fig. 2*B*). Remarkably, treatment with L-T4 reduced D2 activity in a brain structure–specific manner. The most responsive structure was the hippocampus, exhibiting an ~84% drop in D2 activity, trailed by the cerebellum (~72%), striatum (~68%), and cerebral cortex (~17%). Notably, the D2 activity in the hypothalamus was not affected by hypothyroidism or by L-T4 administration (Fig. 2*C*).

To exclude the possibility that the variable D2 response to L-T4 was due to differences in T4 uptake in the brain, we performed intracerebroventricular (*i.c.v*) injection (directly into the lateral cerebral ventricle of the brain) of a single 6 μg dose of L-T4 in THAI mice and measured tissue T4 content 6 h later (Fig. 3*A*). Tissue T4 content increased to similar levels in the cerebral cortex and the hypothalamus (Fig. 3*B*), two relatively distant areas that, as we saw, exhibited very different responses to administration of L-T4 (Fig. 2*C*). We next estimated the impact of the D2 pathway on local T3 signaling by measuring *Luc* mRNA (the T3-induced reporter gene of this model) in these areas. While *Luc* mRNA levels increased ~sevenfold in the mediobasal hypothalamus (MBH), they only increased ~twofold in the cerebral cortex, despite the similar availability of local T4 (Fig. 3*C*). Plotting the *Luc* mRNA vs. tissue T4 levels revealed dramatic differences between these two brain areas in their ability to transduce T4 signaling (Fig. 3*D* and *SI Appendix*, Table S1).

We also considered the possibility that differences in T3 inactivation via the D3 pathway [which is very active in neurons residing in the cerebral cortex of mice (27) and humans (28)] could be involved. After the *i.c.v.* injection of L-T4, *Dio3* induction was much greater in the MBH than in the cerebral cortex, making it unlikely that the enhanced transduction of the T4 signaling was due to slower clearance of TH (Fig. 3*E*). Notably, plotting the expression levels of *Dio3* (which is also inducible by T3) vs. tissue T4 levels showed marked differences between the MBH and the cortex in the transduction of T4 signaling (Fig. 3*F* and *SI Appendix*, Table S1). There was also a strong correlation between *Luc* and *Dio3* both in the MBH and in the cortex (Fig. 3 *G* and *H* and *SI Appendix*, Table S1).

A corollary of these experiments is that the MBH and the cerebral cortex are two brain areas in which D2 activity and D2-mediated T3 signaling exhibit markedly different behaviors when processing T4. These differences are neither the result of variable T4 uptake nor D3-mediated TH inactivation, but rather are due to variable effectiveness of D2-mediated T4 activation to T3. It is conceivable that the ubiquitin–proteasome pathway that processes D2 in these areas plays a major role in this process.

D2 Regulation Is Cell Type Specific: Tanycytes (MBH) vs. Astrocytes (Cerebral Cortex). *Dio2* expression in the MBH is restricted to tanycytes (the astrocytes in MBH do not express *Dio2*), whereas in the cerebral cortex, *Dio2* expression is restricted to astrocytes (29–31). Thus, we hypothesized that differences in T4-induced D2 ubiquitination (and/or proteasomal degradation) between tanycytes and astrocytes would provide a mechanistic explanation for the variable effectiveness of T4 transduction in the MBH and cerebral cortex. To explore this possibility, we established mouse primary cultures of MBH tanycytes and cortical astrocytes (Fig. 4 *A*–*G*). We studied D2 activity in cell sonicates with ^{125}I-T4 using our

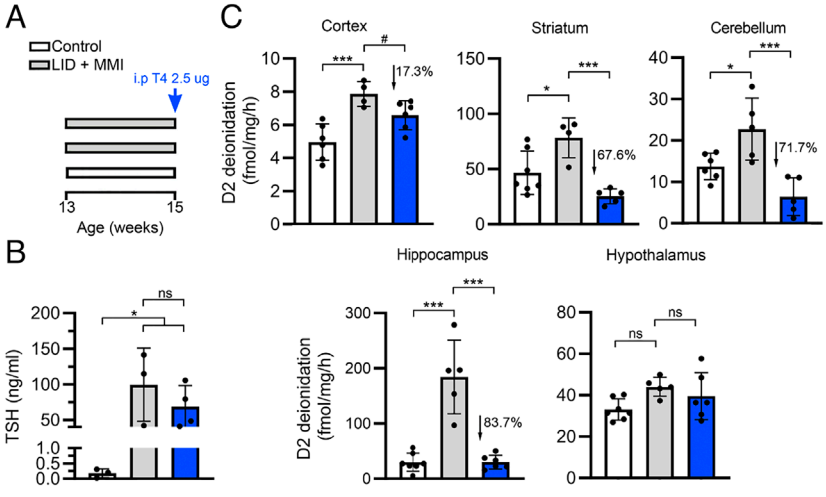

Fig. 2. Different brain areas exhibit variable responses of D2 activity to the treatment of THAI mice with L-T4. (*A*) The diagram shows the experimental groups studied; colored horizontal bars show different treatments. One group (blue bars) was treated intraperitoneally with 2.5 μg of L-T4. (*B*) Plasma TSH in mice undergoing the indicated treatment. (*C*) D2 deiodination (^{125}I-T4 → T3+^{125}I conversion) in the indicated areas and treatments. Treatment with 2.5 μg of L-T4 reduced D2 activity in a region-specific manner. Values are mean ± SD of four to six independent experiments; One-way ANOVA and the Tukey post hoc test were used for multiple comparisons; $^{*}P < 0.05$, $^{***}P < 0.001$; ns: nonsignificant. $^{\#}P < 0.05$ by the *t* test; LID: low iodine diet, MMI: methimazole, TSH: thyrotropine, D2: type 2 deiodinase, i.p T4: intraperitoneal T4 treatment.

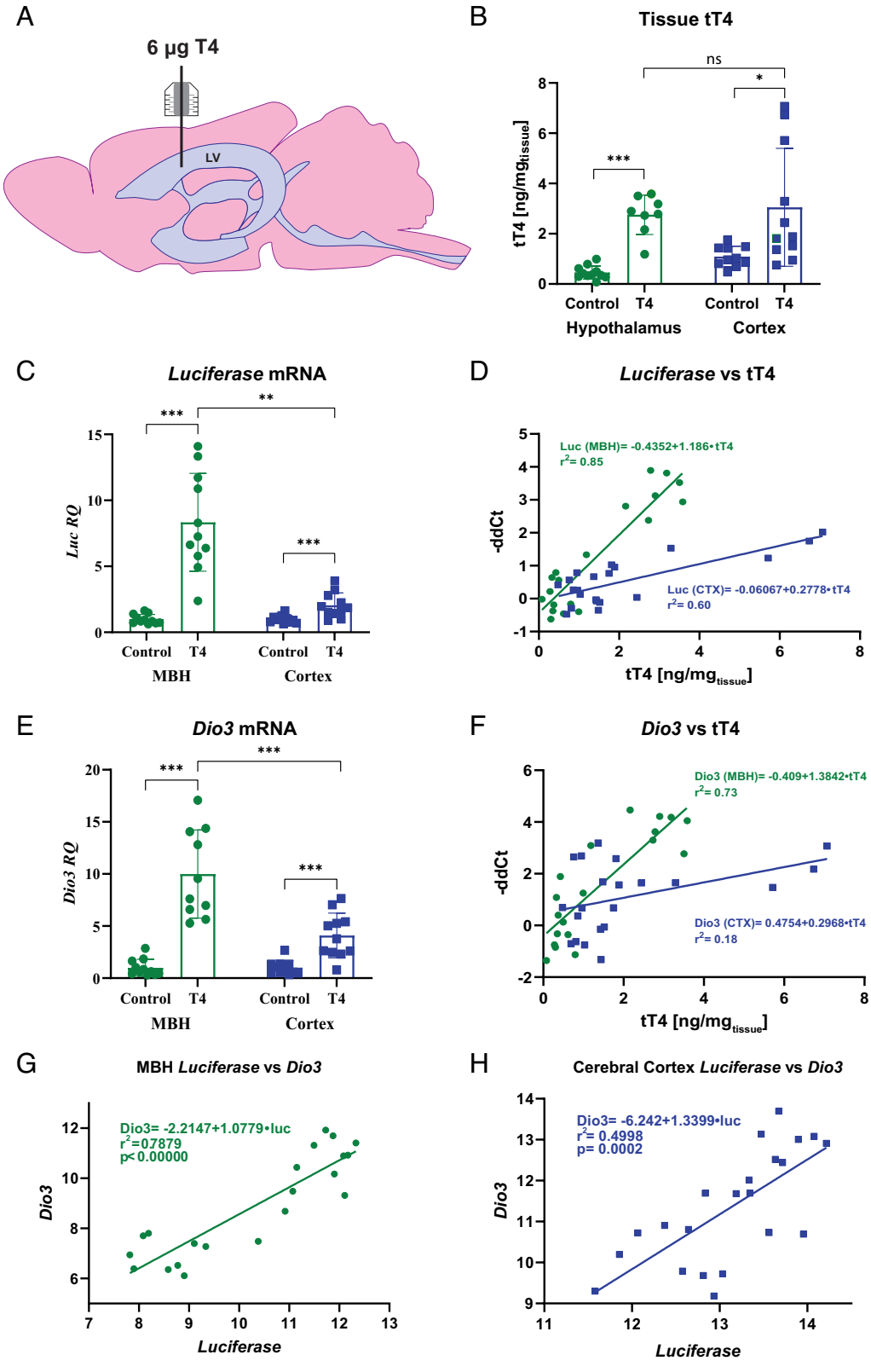

Fig. 3. The mediobasal hypothalamus and the cerebral cortex exhibit different TH signaling to the same tissue level of elevated L-T4. (*A*) Cartoon showing the *i.c.v* injection of L-T4 into the lateral ventricle of THAI mouse. (*B*) Tissue total T4 (tT4) content in the indicated brain regions 6 hours after *i.c.v*. injection of 6 µg L-T4. (*C*) *Luc* mRNA levels. Groups are represented with mean ± SD of 8-11 independent experiments and were analyzed by two-way ANOVA followed by Tukey post-hoc test. (*D*) Linear regression of *Luc* mRNA levels *vs.* tissue T4 content in the cerebral cortex (blue squares) and MBH (green dots). Gene expression data was normalized to the mean of untreated group and multiplied by minus one (-ddCt). One unit increase in –ddCt means a twofold increase in gene expression. The Pearson's correlation coefficient between parameters was higher in the MBH than in the cerebral cortex (r^2 = 0.85 vs 0.60, respectively). (*E*) Same as in (*C*) but for *Dio3*. (*F*) Same as in (*D*) but for *Dio3*. (*G*) Linear regression of *Luc* and *Dio3* mRNA levels in the MBH. (*H*) Same as in (*G*) but in the cerebral cortex. Values are mean ± SD. Differences between the slopes of the regression functions were analyzed using the homogeneity of slopes test. r^2: square of Pearson correlation coefficient. *p <0.05, ***p < 0.001; ns: non-significant; MBH: mediobasal hypothalamus, CTX: cerebral cortex, LV: lateral ventricle, Luc: luciferase, *Dio3*. type 3 deiodinase, T4: thyroxine, tissue tT4: total T4 in tissue homogenate.

established protocol to induce D2 ubiquitination and proteasomal degradation with reverse T3 (rT3) that does not interfere with TH signaling (20, 32). Tanycytes were isolated by microdissecting the MBH of P10 Rax/Cre-Ert2//Gt(ROSA)26Sor_CAG/LSL_ZsGreen1 mice and cultured to select out astrocytes. Rax is a tanycyte-specific marker that induces ZsGreen expression after crossing with the ZsGreen fl/fl mice with Rax-CreERT2 mouse in the presence of tamoxifen (33) (Fig. 4 *A*–*F*). Cerebral cortex astrocytes were isolated from P2-3 mice and visualized with anti-glial fibrillary acidic protein (GFAP) antibodies (Fig. 4*G*).

Cultured astrocytes exhibited ~fivefold higher D2 activity vs. tanycytes (Fig. 4 *H* and *I*). Nonetheless, in the presence of 1 µM rT3 (20, 32), cortical astrocytes lost ~50% of the D2 activity after 90 min, whereas in the tanycytes D2 activity remained stable (Fig. 4 *H* and *I*). This indicates that tanycytes maintain their ability to convert T4 to T3 even as we attempted

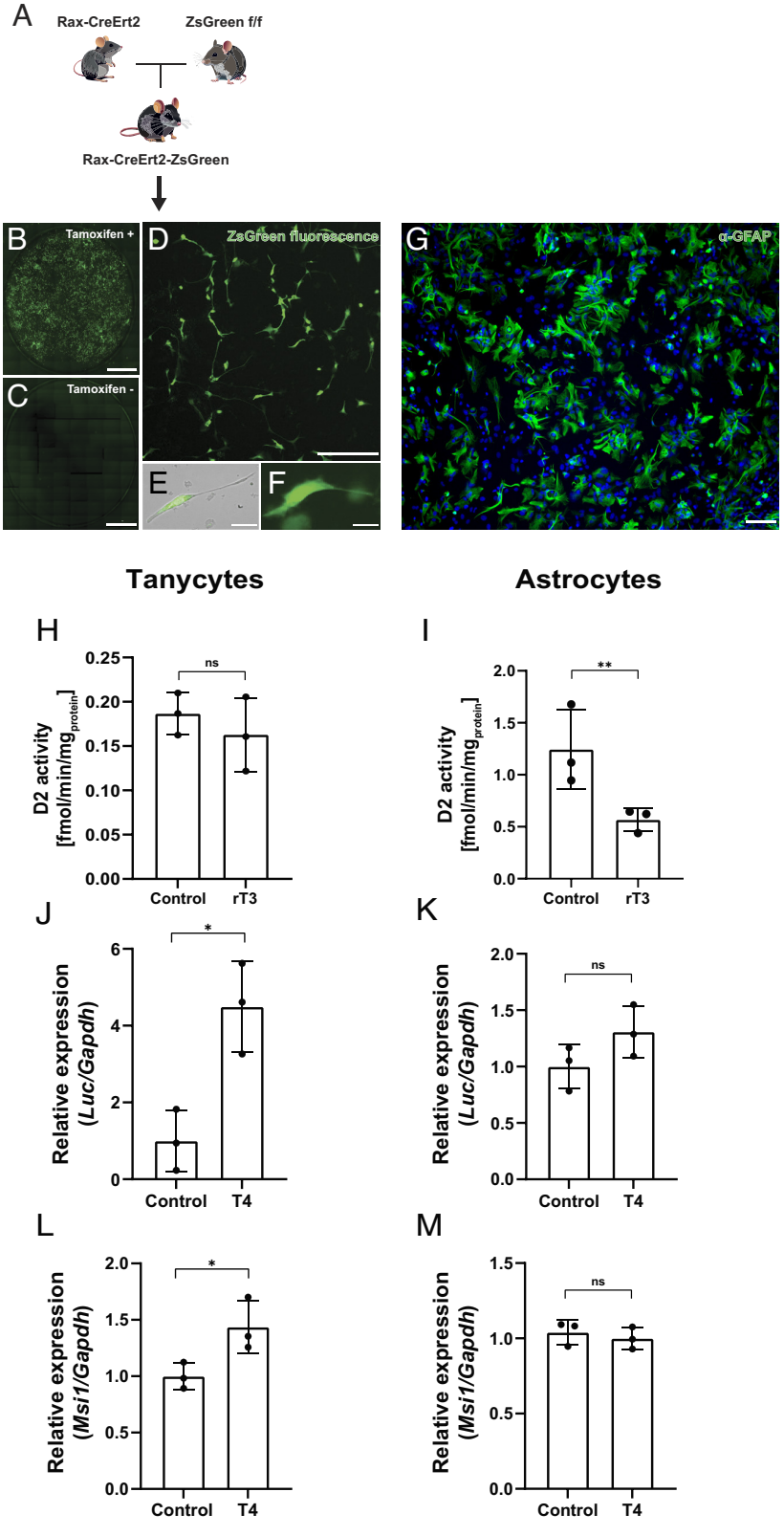

Fig. 4. Modeling T4-induced D2 inactivation in hypothalamic tanycytes and cerebral cortical astrocytes. (*A*) Rax-CreErt2 and ZsGreen mouse lines were crossed to create an animal model expressing a tanycyte-specific marker in the MBH. (*B* and *C*) ZsGreen fluorescent primary tanycytes isolated from Rax-CreErt2 x ZsGreen P10 mice, before (*C*) and 2 d after (*B*) treatment with 1 μM tamoxifen. (*D*) High magnification of ZsGreen fluorescent primary tanycytes. (*E* and *F*) High magnification of cultured tanycytes showing typical morphology. (*G*) Cortical astrocytes isolated from P1-3 mice stained with GFAP (green) and DAPI (blue). (*H*) D2 deiodination (^{125}I-T4 → T3 conversion) in hypothalamic tanycytes at the indicated conditions after treatment with 1 μM rT3 for 1.5 h. (*I*) Same as in (*D*) but for cortical astrocyte cultures. (*J*) *Luc* mRNA expression after treatment with 1 μM T4 for 1.5 h determined by Taqman PCR in tanycyte cultures generated from THAI mice. (*K*) Same as in (*J*) but for cortical astrocyte cultures from THAI mice. (*L*) *Msi1* mRNA expression after treatment with 1 μM T4 for 1.5 h determined by Taqman PCR in tanycyte cultures generated from THAI mice. (*M*) Same as in (*L*) but for cortical astrocyte cultures from THAI mice. Values are mean ± SD of three independent experiments. A two-tailed Student test was used to compare D2 deiodination between conditions; *P < 0.05, **P < 0.01; ns: nonsignificant. Scale bars: (*B* and *C*): 2.5 mm, (*D*): 500 μm (*E*): 20 μm, (*F*): 40 μm, (*G*): 100 μm; rT3: reverse triiodothyronine, T4: thyroxine, D2: type 2 deiodinase, α-GFAP: glial fibrillary acidic protein alpha, *Luc*: luciferase mRNA, *Msi1*: Musashi RNA binding protein 1 mRNA, *Gapdh*: glyceraldehyde-3-phosphate dehydrogenase mRNA.

to trigger D2 ubiquitination/degradation with rT3. Under the same conditions, astrocytes markedly down-regulated T3 production (Fig. 4*I*). This cell-type-specific response of D2-mediated T3 production was also reflected in T3-mediated gene expression. We studied mRNA levels of the T3-responsive *Luc* reporter and *Musashi1 (Msi1)* (34) in cultured tanycytes and cortical astrocytes obtained from THAI mice. In the presence of 1 μM T4, both *Luc* and *Msi1* mRNA increased significantly in tanycytes (Fig. 4 *J* and *K*) but did not respond in astrocytes (Fig. 4 *L* and *M*).

A possibility raised by these results is that, in tanycytes, D2 is less susceptible to ubiquitination and/or proteasomal degradation, as shown in vitro using hypothalamic extracts (35). However, tanycytes are unique in that they coexpress two E3 ubiquitin ligases known to interact with and ubiquitinate D2:WSB1 and MARCH6 (36), suggesting that they are properly equipped to

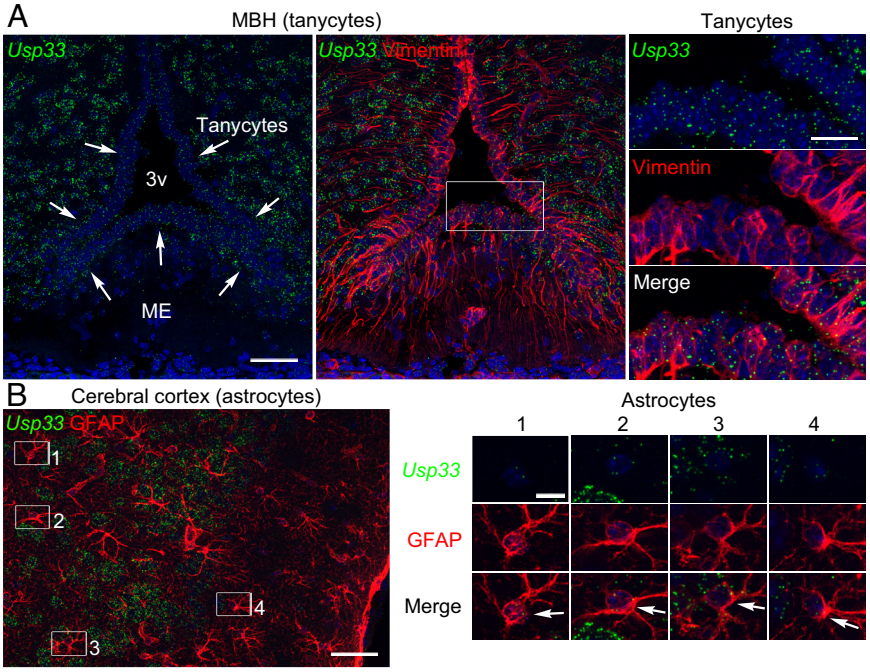

Fig. 5. The USP33 deubiquitinase is abundantly expressed in hypothalamic tanycytes in contrast to cortical astrocytes. (*A*) Fluorescent in situ hybridization shows *Usp33* mRNA (green dots) in the MBH in vimentin-positive tanycytes (red cells) residing in the floor and ventral walls of the third ventricle (limited by arrows). (Scale bar, 50 μm.) *Right* panel: Higher magnification of the *Inset* in the *Middle* panel. (Scale bar, 20 μm.) (*B*) *Usp33* mRNA (green dots) is not expressed in most GFAP-positive cortical astrocytes (red cells). (Scale bar, 50 μm.) *Right* panel: Higher magnification of *Insets* in the *Left* panel shows that only minimal *Usp33* expression can be found in some astrocytes. (Scale bar, 10 μm.) 3V, third ventricle, ME, median eminence, MBH: mediobasal hypothalamus, *Usp33*: ubiquitin-specific peptidase 33 mRNA, GFAP: glial fibrillary acidic protein. DAPI is shown in blue in all panels.

ubiquitinate D2. Indeed, here, we used a Förster Resonance Energy Transfer (FRET)-based approach in HEK293T cells to confirm that even when WSB-1 and MARCH6 are coexpressed (as in the tanycytes), they robustly interact with D2. This critical step is needed for D2 ubiquitination (*SI Appendix*, Fig. S2).

Deubiquitination and Proteasomal Degradation of D2 in Tanycytes and Astrocytes. These findings left us with two alternative explanations for the lack of T4-induced loss of D2 activity in tanycytes: i) tanycytes can rapidly deubiquitinate/reactivate Ub-D2 before it is taken up by the proteasomes and/or ii) tanycytes are limited in their ability to extract Ub-D2 from the endoplasmic reticulum and ship it to the proteasomes.

Ub-D2 can be deubiquitinated by at least two D2-interacting ubiquitin-specific proteases (USPs), i.e., USP20 and USP33, and our earlier studies in rats suggested some level of cell specificity of USP33 expression in the rat brain (37). Therefore, here, we performed fluorescent in situ hybridization combined with immunofluorescence in the mouse brain and visualized tanycytes and cortical astrocytes with vimentin and GFAP, respectively, using laser scanning confocal microscopy. We found high expression levels of *Usp33* in tanycytes while only a very low level was detected in cortical astrocytes (Fig. 5); a sense *Usp33* probe (negative control) did not show labeling (*SI Appendix*, Fig. S3).

Next, we tested the functionality of the Ub-D2 deubiquitination pathway in cortical astrocytes and tanycytes using a mouse with global inactivation of USP33 (USP33-KO). USP33 inactivation was confirmed by undetectable levels of the wild-type *Usp33* mRNA assayed by RT-PCR in the hypothalamus and cerebral cortex (*SI Appendix*, Fig. S4). While D2-activity in USP33-KO astrocytes was similar to that in the control astrocytes (Fig. 6*A*), D2-activity in USP33-KO tanycytes was ~50% lower than in control mice (Fig. 7*A*). This indicates that D2 deubiquitination is a critical pathway in tanycytes and that USP33 does rescue Ub-D2 from terminal degradation in the proteasomes and recycle it into the pool of active D2. However, this is not the case in cortical astrocytes, where D2 activity was not affected by USP33 inactivation. Nonetheless, USP33 inactivation did not change the fact that D2 in tanycytes remained insensitive to rT3 or T4 (Fig. 7 *B* and *C*). This suggests that other USPs, such as USP20, could be reactivating Ub-D2 in tanycytes or that a further downstream process, such as Ub-D2 extraction from the endoplasmic reticulum and transfer to the proteasomes, could be playing a role.

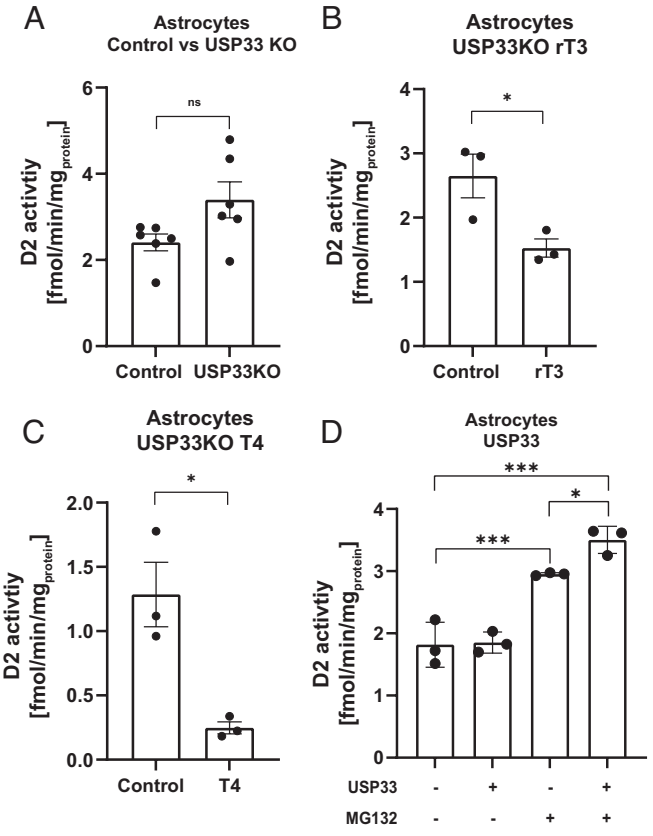

Fig. 6. Studies on D2 deubiquitination and proteasomal degradation in astrocytes. (*A*) D2 activity in astrocytes from the indicated mice. (*B*) D2 activity in USP33KO astrocytes with rT3 (0.5 μM, 1.5 h) treatment. (*C*) D2 activity in USP33KO astrocytes with T4 treatment (0.5 μM, 1.5 h). (*D*) D2 activity in wild-type astrocytes with or without transfected USP33 and proteasomal uptake inhibitor MG132 (10 μM; incubation time 1.5 h). Values are mean ± SD. A two-tailed Student test was used to compare D2 activity between two conditions, one-way ANOVA followed by the Tukey post hoc test was used to compare multiple conditions; *$P < 0.05$; ***$P < 0.001$; ns: nonsignificant; D2: type 2 deiodinase, rT3: reverse triiodothyronine, T4: thyroxine, KO: knock out, USP33: ubiquitin-specific peptidase 33.

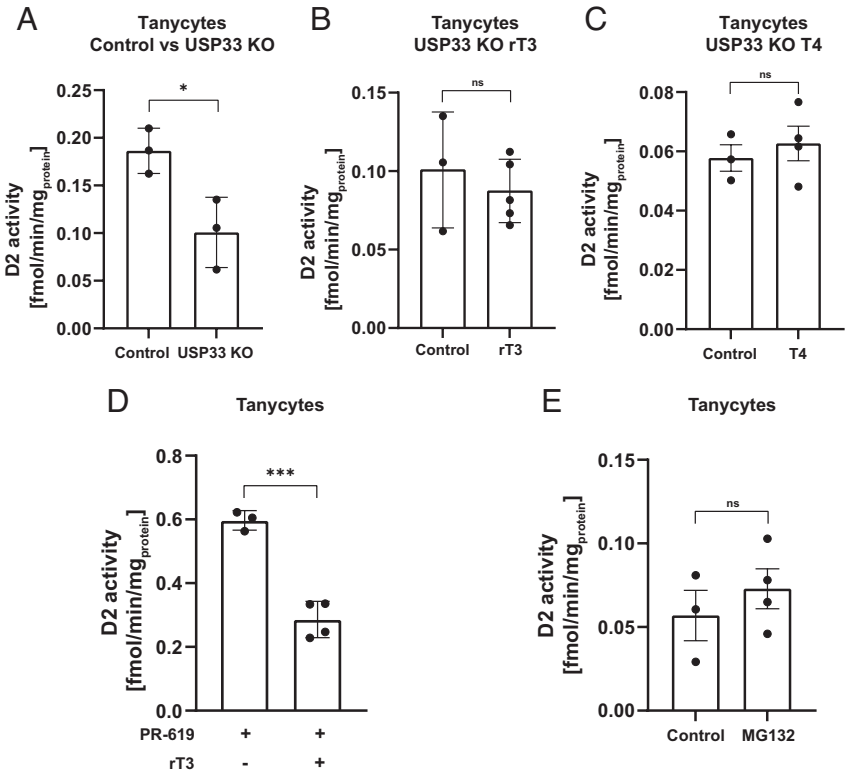

Fig. 7. Studies on D2 deubiquitination and proteasomal degradation in tanycytes. (*A*) D2 activity in tanycytes from USP33-KO and control mice. (*B*) D2 activity in USP33KO tanycytes after rT3 treatment (1 μM, 1.5 h). (*C*) D2 activity in USP33KO tanycytes after T4 treatment (1 μM, 1.5 h). (*D*) D2 activity in wild-type tanycytes treated with the deubiquitinase inhibitor [2,6-Diamino-3,5-dithiocyanopyridine (PR-619) (4 μM; incubation time 24 h) and rT3 (1 μM for the final 1.5 h of PR-619 treatment)]. (*E*) D2 activity in wild-type tanycytes treated with proteasomal uptake inhibitor MG132 (10 μM; incubation time 1.5 h). Values are mean ± SD. A two-tailed Student test was used to compare D2 activity between conditions; **P* < 0.05; ****P* < 0.001; ns: nonsignificant; D2: type 2 deiodinase, rT3: reverse triiodothyronine, T4: thyroxine, KO: knock out, USP33: ubiquitin-specific peptidase 33.

These possibilities were tested by treating tanycytes with 2,6-Diamino-3,5-dithiocyanopyridine (PR-619), a broad-range deubiquitinase inhibitor that inhibits various USPs (38). Importantly, in the presence of PR-619, exposure to rT3 induced a ~50% loss of D2 activity in tanycytes (Fig. 7*D*), a response that was indistinguishable from that observed in astrocytes (Fig. 4*I*). In addition, tanycytes and cortical astrocytes were treated with the proteasomal inhibitor MG132. Typically, such treatment increases D2 activity by twofold in a few hours (20, 32). Here, treatment with MG132 increased D2 activity in astrocytes by ~50%, regardless of the presence or absence of overexpressed USP33 (Fig. 6*D*). This confirms that D2 is ubiquitinated and actively taken up by the proteasomes in these cells. In contrast, treatment of tanycytes with MG132 did not increase D2 activity, confirming that in these cells, proteasomal degradation of Ub-D2 is not an active pathway (Fig. 7*E*).

Discussion

A fundamental principle governing our understanding of TH homeostasis is that D2-mediated T4 activation to T3 is self-limited. This mechanism curbs T3 production by D2 ubiquitination and degradation in the proteasomes (20). We recently uncovered evidence that the effectiveness of this autoregulatory mechanism is site specific. It is very effective in skeletal muscle and bone marrow, but almost nonexistent in the pituitary gland (23). In the present investigation, we observed that also in tanycytes residing in the MBH, there is almost no limitation in the T4 activation to T3. Furthermore, we provide a molecular explanation for why this is the case. Intense deubiquitination of Ub-D2 and limited proteasomal uptake of Ub-D2 in tanycytes explain why fluctuations in plasma T4 levels are faithfully transduced into local T3 signaling, modulating TRH and TSH secretion. The fact that this self-limiting mechanism is site specific led us to study TH signaling in the brain of L-T4-treated mice. Our mouse model replicates the higher plasma T4, lower plasma T3, and normal TSH levels observed in L-T4-treated patients. We found that the transduction of T4 signaling in the brain of these mice is also uneven and depends on the brain structure analyzed (Fig. 8).

In some brain structures, such as the MBH, the D2 self-limiting mechanism is almost absent, allowing for sustained T3 production and a much stronger induction of the T3-reporter gene. Deubiquitination and impaired proteasomal uptake of Ub-D2 in tanycytes (as opposed to astrocytes) are two major differences that can explain this unusual D2 behavior in tanycytes (39). These findings suggest that normalization of T3 signaling in all brain areas of L-T4-treated patients could be difficult to achieve. This is concerning, given that some L-T4-treated patients do exhibit cognitive impairment despite normalization of TSH (4, 40–42).

Unfortunately, one of the by-products of L-T4 monotherapy is an elevation in plasma T4 levels, which in many tissues (but not all) forces D2 ubiquitination and limits T3 production. It is estimated that up to 40% of the L-T4-treated patients have serum-free T4 levels above the upper limit of normal, despite exhibiting normal serum TSH levels (24, 43). The fact that brain structures activate T4 with different efficiencies explains why T3 signaling in the cerebellum of L-T4-treated mice remained suboptimal while it had been normalized in the cerebral cortex, hippocampus, and striatum. It is notable that higher doses of L-T4 restored T3 signaling in the cerebellum but slightly elevated TH signaling in the cerebral cortex.

The inability of the deiodinase pathway to compensate for high plasma T4 levels is not unexpected. No situation in nature is associated with elevated plasma T4 levels, hence the poor adaptive response. In contrast, the thyroid system is fully prepared to deal with low plasma T4 levels. This is because iodine availability is the strongest evolutionary pressure shaping the thyroid gland and the deiodinases' evolution. Iodine deficiency lowers plasma T4 levels but the T3 levels remain stable (21, 22) thanks to higher serum TSH levels [which increases the T3/T4 ratio in the thyroid secretion (44)] and to an accelerated T4 to T3 conversion via the D2 pathway (45). The latter directly results from less T4-induced D2 ubiquitination/proteasomal degradation, which prolongs D2 half-life (20, 39).

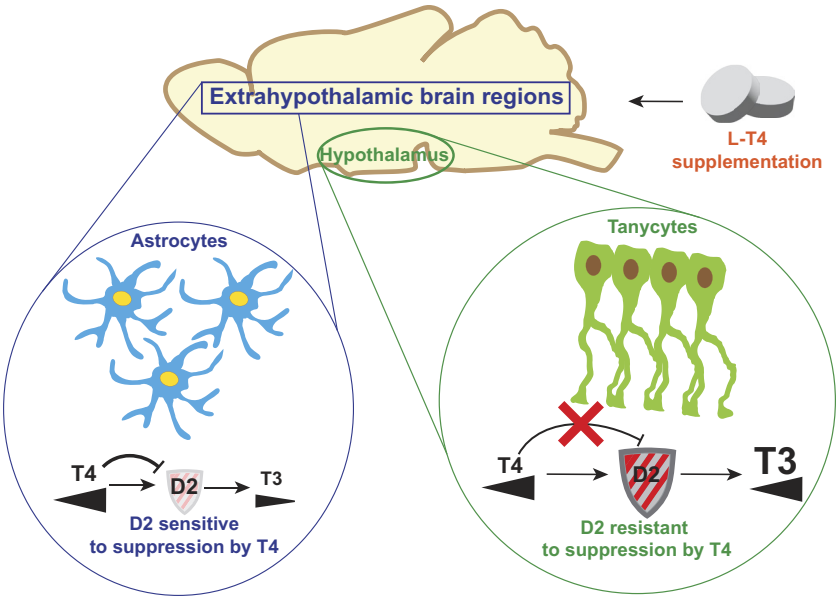

Fig. 8. Schematic cartoon summarizing the main findings. Excessive L-T4-supplementation exerts brain structure–specific effects on the local TH action of the brain. D2 in hypothalamic tanycytes is protected from T4-induced inactivation, while astrocytic D2 in other brain regions is not. These differences are due to cell-type-specific differences in D2 deubiquitination. Therefore, amid supraphysiological L-T4 exposure, the hypothalamic D2 efficiently produces T3 while extrahypothalamic brain regions face suboptimal TH signaling; L-T4: thyroxine supplement, T4: thyroxine, T3: triiodothyronine, D2: type 2 deiodinase.

The present investigation gave us a much better insight into the mechanistic underpinning of the variable effectiveness of the D2-mediated T4 activation to T3 in the brain. First, we saw that tanycytes are equipped to ubiquitinate D2 as they uniquely coexpress two bonafide E3 ubiquitin ligases WSB1 and MARCH6 (36). Through modeling the tanycyte-specific coexpression of D2 with WSB1 and MARCH6 in HEK293T cells we found that both E3 ligases physically interact with D2 and do not interfere with each other or with the known conformational changes of the D2+T4 → Ub-D2+T3+I pathway (46).

Second, we found that the mouse tanycytes are unique in the brain in that they abundantly express USP33, which is not the case in astrocytes. We worked with primary cultures of MBH tanycytes and cerebral cortical astrocytes and noticed that the differences in TH-induced loss of D2 activity reflected what we had observed in the in vivo experiments. Tanycytes showed resilience to substrate-induced activity loss (by either rT3 or T4), while in contrast, treatment with high doses of substrate resulted in a ~50% drop in D2 activity in astrocytes and this cell-type-specific difference was reflected in T3-dependent gene expression. Furthermore, USP33 inactivation halved D2 activity in tanycytes. This is because Ub-D2 is rescued by USP33-mediated deubiquitination and this prevents D2 from being pulled from the ER membrane and directed to the proteasome system (47). However, despite the strong functionality of this pathway in tanycytes, USP33 inactivation was not sufficient to make tanycytes behave as astrocytes in terms of T4-induced loss of D2 activity. USP33-KO tanycytes continued to convert T4 to T3 at a steady pace, even in the presence of an excess of T4. The existence of other USPs that bind to and deubiquitinate D2, such as USP20 (48), USP10, and USP14, could provide a redundant pathway for Ub-D2 deubiquitination (49, 50). Our finding that PR-619, a broad-range deubiquitinase inhibitor (38) led tanycytes to behave as astrocytes in terms of T4-induced loss of D2 activity demonstrated the decisive role of cell-type-specific regulation of D2-ubiquitination in response to T4.

Third, we saw that inhibiting the proteasomes with MG132 does not increase D2 activity in tanycytes. This is a critical finding as it indicates that in tanycytes, the removal of Ub-D2 from the ER and its transfer to the proteasomes might not be an active pathway. It is conceivable that the variable effectiveness of treatment with L-T4 to restore TH signaling in all brain structures is the result of differences in the functionality of these three mechanisms among astrocytes in different brain structures.

The clinical implications of these findings should not be underestimated. The high prevalence of above-normal T4 levels in L-T4-treated patients sets the stage for multiple levels of TH signaling in the brains of these patients, possibly explaining their residual cognitive symptoms. In addition, to improve the effectiveness of therapy with L-T4, it is common practice among clinicians to adjust the dose of L-T4 up to bring TSH levels closer to the lower limit of normal. The present studies revealed that this approach might be beneficial to certain structures of the brain but detrimental to others.

The present investigation provided yet an even more clear understanding of how the T4-mediated TSH feedback mechanism operates. The existence of the self-limiting D2-mediated T3 production was counterintuitive (51). How could fluctuations in plasma T4 be faithfully transduced to the TRH-TSH-secreting cells if T3 production was limited by D2 degradation in the proteasomes? We first obtained evidence of steady T3 production (reduced D2 self-limiting mechanism) in tumor cell lines secreting TSH (51), and later in pituitary gland explants (23). Here, we completed the picture by including the tanycytes and identified the role of D2 deubiquitination and impaired proteasomal uptake in this process. It is then likely that in L-T4-treated patients, an elevation in T4 levels from 10 to 20 pM causes TSH to drop by 10-fold (52) simply because there is no self-limiting D2 mechanism in the tanycytes and the pituitary gland. In contrast, the same patients continue to exhibit steady T3 levels (52) because of the existing self-limiting mechanism in the periphery that limits T3 production.

In conclusion, here, we provide evidence that the efficiency of the activation of T4 to T3 via D2 varies according to the brain's anatomical site. This is because the efficiency of the self-limiting mechanism that curbs T3 production in the face of an elevating plasma T4 varies among cells. Deubiquitination of Ub-D2 and proteasomal uptake of Ub-D2 are some of the limiting steps that distinguish the D2 pathway in astrocytes and tanycytes, but other differences may exist as well. While the heterogeneity in the transduction of T4 signaling is physiological and explains the T4-mediated TSH feedback mechanism, it may also prove to be maladaptive for patients with hypothyroidism who are treated with L-T4. The resulting elevation in plasma T4 is transduced differently in brain structures of L-T4-treated patients, setting the stage for uneven normalization of T3 signaling and persistent cognitive symptoms.

Materials and Methods

All experiments were approved by the Institutional Animal Care and Use Committee at the University of Chicago (#72577) or by the Animal Welfare Committee at the HUN-REN Institute of Experimental Medicine, Hungary (PE/EA/00865-6/2022, MÁB-1/2021). We followed the American Thyroid Association Guide to Investigating TH Economy and Action in Rodents and Cell Models (53).

Animals. Mice were housed under standard, temperature-controlled conditions with automated light and dark cycles and fed ad libitum with chow diet. THAI and Rax-CreErt2 strains were bred in-house, ZsGreen strain was obtained from The Jackson Laboratory (strain number: 007906), and C57Bl6/J mice were acquired from Charles River Laboratories. Unless otherwise specified, 8- to 10-wk-old male THAI mice were used throughout experiments. The USP33KO C57Bl/6 mice lack the exons 5 to 11 of the USP33 gene and were obtained from GemPharmatech Co., Ltd. (Nanjing, China). Treatment details are given in *SI Appendix*.

TaqMan Real-Time Quantitative PCR. The measurements were performed as previously described (34, 54). The expression of *Luc, Dio3, and MsiI* was detected using a specific TaqMan probe as described (17, 25, 34). Details are given in *SI Appendix* including probe details in *SI Appendix*, Table S2.

Determination of TSH, T3, and T4 Concentrations. TSH was measured by the MILLIPLEX bead panel (Millipore Corporation), and T4 and T3 plasma concentrations were obtained by radioimmunoassay while total tissue T4 concentrations were determined by AccuLite CLIA Microwells kit according to the manufacturer's instructions. Details are given in *SI Appendix*.

Determination of D2-Mediated Deiodination. D2 deiodination in sonicates of brain regions and cell cultures was measured in the presence of 10 mM dithiothreitol, 1 mM propylthiouracil, 0.25 M sucrose, 1 nM T4 (~100.000 to 250,000 cpm ^{125}I-T4), and 10 nM T3, as described (53). Details are given in *SI Appendix*.

Primary Cultures of Tanycytes and Astrocytes. Tanycytes were cultured as described with modifications (55). Cells were isolated from postnatal day 10 (P10) mice as indicated on the figures; pups were decapitated followed by the dissection of the MBH.

Astrocytes were isolated from P1–3 mice as indicated in the figures and legends. Cultures were prepared using standard methods. Experiments on both cell types were performed after 7 d in culture of (~80% confluency). Culture conditions and treatments are detailed in *SI Appendix* and in the legends.

Fluorescent In Situ Hybridization Combined with Immunofluorescence. Adult male C57Bl6/J (15-wk-old) mice were anesthetized, and the brains were removed and frozen. Sections were prepared on cryostat and then hybridized with a digoxigenin-labeled antisense Usp33 riboprobe, corresponding to 414 to 1306 bases of the mouse *Usp33* mRNA (GenBank #NM_133247). The hybridization signal was amplified with the TSA Plus Biotin Kit followed by detection of biotin deposits with Alexa Fluor 488–conjugated Streptavidin. Sections were incubated with a rabbit monoclonal antibody against vimentin or with a mouse monoclonal antibody against GFAP followed by detection with Alexa Fluor 555–conjugated anti-rabbit or anti-mouse IgG, respectively. Images were obtained with a Zeiss LSM 780 confocal microscope. Details are given in *SI Appendix*.

FRET. To examine the interaction between the proteins D2, WSB1, and MARCH6, we used a modified method of our previously established protocols (46, 56). The interactions between D2, WSB1, and MARCH6 were calculated using the sequential acceptor photobleaching method (56). Details are given in *SI Appendix*.

Data Analysis. All data were analyzed using PRISM software (GraphPad Software 9.5.1, Inc) and STATISTICA V14 and expressed as mean ± SD. The Student *t* test was used to compare two groups. Multiple group comparisons were done using ANOVA models, which are detailed in figure legends. The correlation coefficient (r^2) refers to the square of the Pearson correlation coefficient. Simple linear regression and the Pearson correlation coefficient were used to analyze the connection between gene expression data and tissue T4. Regression models were compared with homogeneity of slopes test. Significance was set at $P < 0.05$ to reject the null hypothesis.

Data, Materials, and Software Availability. All study data are included in the article and/or *SI Appendix*.

ACKNOWLEDGMENTS. We are grateful for support from National Institute of Diabetes and Digestive and Kidney Diseases (DK58538) and the National Research, Development and Innovation Office of Hungary (RRF-2.3.1-21-2022-00011). The technical help of Andrea Juhász is gratefully acknowledged. The Rax-CreERT2 mouse was kindly provided by Dr. S. Blackshaw (Baltimore, MD).

Author affiliations: [a]Laboratory of Molecular Cell Metabolism, HUN-REN Institute of Experimental Medicine, Budapest 1083, Hungary; [b]Section of Adult and Pediatric Endocrinology and Metabolism, University of Chicago, Chicago, IL IL60637; [c]János Szentágothai Neurosciences Division, Doctoral College, Semmelweis University, Budapest 1085, Hungary; and [d]Laboratory of Integrative Neuroendocrinology, HUN-REN Institute of Experimental Medicine, Budapest 1083, Hungary

1. L. Chaker, A. C. Bianco, J. Jonklaas, R. P. Peeters, Hypothyroidism. *Lancet* **390**, 1550–1562 (2017).
2. L. Hegedus *et al.*, Primary hypothyroidism and quality of life. *Nat. Rev. Endocrinol.* **18**, 230–242 (2022).
3. M. D. Ettleson *et al.*, Brain fog in hypothyroidism: Understanding the patient's perspective. *Endocr. Pract.* **28**, 257–264 (2022).
4. S. Casula, M. D. Ettleson, A. C. Bianco, Are we restoring thyroid hormone signaling in levothyroxine-treated patients with residual symptoms of hypothyroidism? *Endocr. Pract.* **29**, 581–588 (2023).
5. C. P. Marcelino *et al.*, Temporal pole responds to subtle changes in local thyroid hormone signaling. *J. Endocr. Soc.* **4**, bvaa136 (2020).
6. J. Bernal, Thyroid hormones and brain development. *Vitam Horm* **71**, 95–122 (2005).
7. A. C. Bianco *et al.*, Paradigms of dynamic control of thyroid hormone signaling. *Endocr. Rev.* **40**, 1000–1047 (2019).
8. F. Salas-Lucia, Mapping thyroid hormone action in the human brain. *Thyroid* **34**, 815–826 (2024).
9. B. Gereben *et al.*, Cellular and molecular basis of deiodinase-regulated thyroid hormone signaling. *Endocr. Rev.* **29**, 898–938 (2008).
10. F. Salas-Lucia *et al.*, Axonal T3 uptake and transport can trigger thyroid hormone signaling in the brain. *Elife* **12**, e82683 (2023).
11. B. Morte, J. Bernal, Thyroid hormone action: Astrocyte-neuron communication. *Front. Endocrinol. (Lausanne)* **5**, 82 (2014).
12. J. Bernal, A. Guadano-Ferraz, B. Morte, Thyroid hormone transporters-functions and clinical implications. *Nat. Rev. Endocrinol.* **11**, 690 (2015).
13. F. R. Crantz, J. E. Silva, P. R. Larsen, Analysis of the sources and quantity of 3,5,3′-triiodothyronine specifically bound to nuclear receptors in rat cerebral cortex and cerebellum. *Endocrinology* **110**, 367–375 (1982).
14. P. Mohacsik, A. Zeold, A. C. Bianco, B. Gereben, Thyroid hormone and the neuroglia: Both source and target. *J. Thyroid Res.* **2011**, 215718 (2011).
15. B. C. Freitas *et al.*, Paracrine signaling by glial cell-derived triiodothyronine activates neuronal gene expression in the rodent brain and human cells. *J. Clin. Invest.* **120**, 2206–2217 (2010).
16. B. M. Bocco *et al.*, Type 2 deiodinase disruption in astrocytes results in anxiety-depressive-like behavior in male mice. *Endocrinology* **157**, 3682–3695 (2016).
17. R. Sinko *et al.*, Different hypothalamic mechanisms control decreased circulating thyroid hormone levels in infection and fasting-induced non-thyroidal illness syndrome in male thyroid hormone action indicator mice. *Thyroid* **33**, 109–118 (2023).
18. E. A. McAninch *et al.*, Prevalent polymorphism in thyroid hormone-activating enzyme leaves a genetic fingerprint that underlies associated clinical syndromes. *J. Clin. Endocrinol. Metab.* **100**, 920–933 (2015).
19. A. Ceballos *et al.*, Importance of monocarboxylate transporter 8 for the blood-brain barrier-dependent availability of 3,5,3′-triiodo-L-thyronine. *Endocrinology* **150**, 2491–2496 (2009).
20. B. Gereben, C. Goncalves, J. W. Harney, P. R. Larsen, A. C. Bianco, Selective proteolysis of human type 2 deiodinase: A novel ubiquitin- proteasomal mediated mechanism for regulation of hormone activation. *Mol. Endocrinol.* **14**, 1697–1708 (2000).
21. I. J. Chopra, J. M. Hershman, R. W. Hornabrook, Serum thyroid hormone and thyrotropin levels in subjects from endemic goiter regions of New Guinea. *J. Clin. Endocrinol. Metab.* **40**, 326–333 (1975).
22. J. T. Nicoloff, S. M. Lum, C. A. Spencer, R. Morris, Peripheral autoregulation of thyroxine to triiodothyronine conversion in man. *Horm Metab. Res. Suppl.* **14**, 74–79 (1984).
23. A. Batistuzzo, F. Salas-Lucia, B. Gereben, M. O. Ribeiro, A. C. Bianco, Sustained pituitary T3 production explains the T4-mediated TSH feedback mechanism. *Endocrinology* **164**, bqad155 (2023).
24. G. C. Penna, I. M. Bensenor, A. C. Bianco, M. D. Ettleson, Thyroid hormone homeostasis in levothyroxine-treated patients: Findings from ELSA-Brasil. *J. Clin. Endocrinol. Metab.* **109**, 2504–2512 (2024), 10.1210/clinem/dgae139.
25. P. Mohacsik *et al.*, A transgenic mouse model for detection of tissue-specific thyroid hormone action. *Endocrinology* **159**, 1159–1171 (2018).
26. J. Jonklaas *et al.*, Guidelines for the treatment of hypothyroidism: Prepared by the american thyroid association task force on thyroid hormone replacement. *Thyroid* **24**, 1670–1751 (2014).
27. A. Hernandez, B. Morte, M. M. Belinchon, A. Ceballos, J. Bernal, Critical role of types 2 and 3 deiodinases in the negative regulation of gene expression by T(3)in the mouse cerebral cortex. *Endocrinology* **153**, 2919–2928 (2012).
28. F. Salas-Lucia, S. Escamilla, A. C. Bianco, A. Dumitrescu, S. Refetoff, Impaired T3 uptake and action in MCT8-deficient cerebral organoids underlie Allan-Herndon-Dudley syndrome. *JCI Insight* **9**, e174645 (2024).
29. C. Fekete *et al.*, DARPP-32 and CREB are present in type 2 iodothyronine deiodinase- producing tanycytes: Implications for the regulation of type 2 deiodinase activity. *Brain Res.* **862**, 154–161 (2000).
30. T. L. Fonseca *et al.*, Coordination of hypothalamic and pituitary T3 production regulates TSH expression. *J. Clin. Invest.* **123**, 1492–1500 (2013).

31. A. Guadano-Ferraz, M. J. Obregon, D. L. St Germain, J. Bernal, The type 2 iodothyronine deiodinase is expressed primarily in glial cells in the neonatal rat brain. *Proc. Natl. Acad. Sci. U.S.A.* **94**, 10391–10396 (1997).
32. M. Dentice *et al.*, The Hedgehog-inducible ubiquitin ligase subunit WSB-1 modulates thyroid hormone activation and PTHrP secretion in the developing growth plate. *Nat. Cell Biol.* **7**, 698–705 (2005).
33. T. Pak, S. Yoo, A. L. Miranda-Angulo, H. Wang, S. Blackshaw, Rax-CreERT2 knock-in mice: A tool for selective and conditional gene deletion in progenitor cells and radial glia of the retina and hypothalamus. *PLoS One* **9**, e90381 (2014).
34. P. Mohacsik *et al.*, The Musashi-1-type 2 deiodinase pathway regulates astrocyte proliferation. *J. Biol. Chem.* **300**, 107477 (2024).
35. J. P. Werneck de Castro *et al.*, Differences in hypothalamic type 2 deiodinase ubiquitination explain localized sensitivity to thyroxine. *J. Clin. Invest.* **125**, 769–781 (2015).
36. A. M. Zavacki *et al.*, The E3 ubiquitin ligase TEB4 mediates degradation of type 2 iodothyronine deiodinase. *Mol. Cell Biol.* **29**, 5339–5347 (2009).
37. C. Fekete *et al.*, Expression patterns of WSB-1 and USP-33 underlie cell-specific posttranslational control of type 2 deiodinase in the rat brain. *Endocrinology* **148**, 4865–4874 (2007).
38. M. Altun *et al.*, Activity-based chemical proteomics accelerates inhibitor development for deubiquitylating enzymes. *Chem. Biol.* **18**, 1401–1412 (2011).
39. B. Gereben, E. A. McAninch, M. O. Ribeiro, A. C. Bianco, Scope and limitations of iodothyronine deiodinases in hypothyroidism. *Nat. Rev. Endocrinol.* **11**, 642–652 (2015).
40. P. Saravanan *et al.*, Psychological well-being in patients on "adequate" doses of l-thyroxine: Results of a large, controlled community-based questionnaire study. *Clin. Endocrinol. (Oxf)* **57**, 577–585 (2002).
41. E. A. McAninch, A. C. Bianco, The swinging pendulum in Treatment for hypothyroidism: From (and toward?) combination therapy. *Front. Endocrinol. (Lausanne)* **10**, 446 (2019).
42. S. J. Peterson *et al.*, An online survey of hypothyroid patients demonstrates prominent dissatisfaction. *Thyroid* **28**, 707–721 (2018).
43. D. Gullo *et al.*, Levothyroxine monotherapy cannot guarantee euthyroidism in all athyreotic patients. *PLoS One* **6**, e22552 (2011).
44. P. Laurberg, Mechanisms governing the relative proportions of thyroxine and 3,5,3′-triiodothyronine in thyroid secretion. *Metabolism* **33**, 379–392 (1984).
45. R. Peeters *et al.*, Regional physiological adaptation of the central nervous system deiodinases to iodine deficiency. *Am. J. Physiol. Endocrinol. Metab.* **281**, E54–E61 (2001).
46. G. D. Sagar *et al.*, Ubiquitination-induced conformational change within the deiodinase dimer is a switch regulating enzyme activity. *Mol. Cell Biol.* **27**, 4774–4783 (2007).
47. E. D. R. Arrojo, P. Egri, S. Jo, B. Gereben, A. C. Bianco, The type II deiodinase is retrotranslocated to the cytoplasm and proteasomes via p97/Atx3 complex. *Mol. Endocrinol.* **27**, 2105–2115 (2013).
48. C. Curcio-Morelli *et al.*, Deubiquitination of type 2 iodothyronine deiodinase by von Hippel-Lindau protein-interacting deubiquitinating enzymes regulates thyroid hormone activation. *J. Clin. Invest.* **112**, 189–196 (2003).
49. Y. Bai, Q. Chen, Y. Li, A single-cell transcriptomic study of heterogeneity in human embryonic tanycytes. *Sci. Rep.* **14**, 15384 (2024).
50. E. Sjostedt *et al.*, An atlas of the protein-coding genes in the human, pig, and mouse brain. *Science* **367**, eaay5947 (2020).
51. M. A. Christoffolete *et al.*, Atypical expression of type 2 iodothyronine deiodinase in thyrotrophs explains the thyroxine-mediated pituitary thyrotropin feedback mechanism. *Endocrinology* **147**, 1735–1743 (2006).
52. M. D. Ettleson *et al.*, Serum thyrotropin and triiodothyronine levels in levothyroxine-treated patients. *J. Clin. Endocrinol. Metab.* **108**, e258–e266 (2023).
53. A. C. Bianco *et al.*, American thyroid association guide to investigating thyroid hormone economy and action in rodent and cell models. *Thyroid* **24**, 88–168 (2014).
54. F. Salas-Lucia *et al.*, Effect of the fetal THRB genotype on the placenta. *J. Clin. Endocrinol. Metab.* **108**, e944–e948 (2023).
55. P. N. De Francesco *et al.*, A simple strategy for culturing morphologically-conserved rat hypothalamic tanycytes. *Cell Tissue Res.* **369**, 369–380 (2017).
56. P. Egri, B. Gereben, Minimal requirements for ubiquitination-mediated regulation of thyroid hormone activation. *J. Mol. Endocrinol.* **53**, 217–226 (2014).